Supporting Information for

Computational Identification of Possible Allosteric Sites and Modulators of the SARS-CoV-2 Main Protease

*Debarati DasGupta[1], Wallace K. B. Chan,[2] Heather A. Carlson[1]**

1- Department of Medicinal Chemistry, University of Michigan, Ann Arbor, Michigan 48109-1065, USA.
2- Department of Pharmacology, University of Michigan, Ann Arbor, Michigan 48109-5632, USA

* carlsonh@umich.edu

1. Supporting Figures

- **Figure S1.** Predicted Allosteric Sites on Main Protease using Probeview
- **Figure S2.**: Normal Mode Analysis of Site 1
- **Figure S3.**: Normal Mode Analysis of Site 2
- **Figure S4.**: Normal Mode Analysis of Site 3
- **Figure S5.**: Normal Mode Analysis of Site 4
- **Figure S6.**: Normal Mode Analysis of Site 5
- **Figure S7.**: Normal Mode Analysis of Site 6
- **Figure S8.** Dynamic cross-correlation plot of the pyrimidine MixMD trajectory
- **Figure S9.** Dynamic cross-correlation plot of the isopropanol MixMD trajectory
- **Figure S10.** Dynamic cross-correlation plot of the acetonitrile MixMD trajectory
- **Figure S11.**: Best-binder in allosteric site 1 RMSD fluctuations as a function of time
- **Figure S12.** Best-binder in allosteric site 2 RMSD fluctuations as a function of time
- **Figure S13.** Best-binder allosteric site 3 RMSD fluctuations as a function of time
- **Figure S14.** Protein backbone RMSD fluctuations plotted during the 1-μs simulations of the allosteric-site binders (A) site 1, (B) site 2, and (C) site 3.

2. Supporting Tables

- Scores for the 361 dockable compounds are in Excel_sheet named NCATS_data.xlsx (separate file)

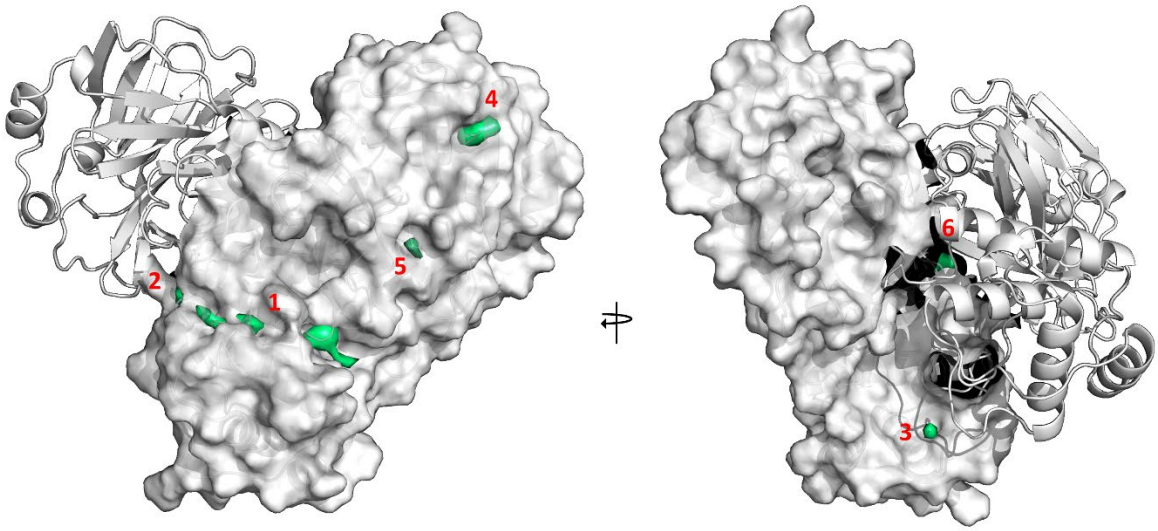

Figure S1. Predicted Allosteric Sites on Main Protease using Probeview. The 6 predicted sites are shown as green surfaces for one monomer (surface representation) for clarity. Sites 1, 2, 4, and 5 lie on the surface of one side of the enzyme (left panel), while Site 3 sits at the bottom of the enzyme (right panel); these all have corresponding sites on the other monomer. Conversely, Site 6 lies between the monomers and thus exists as a single site on the dimer (right panel).

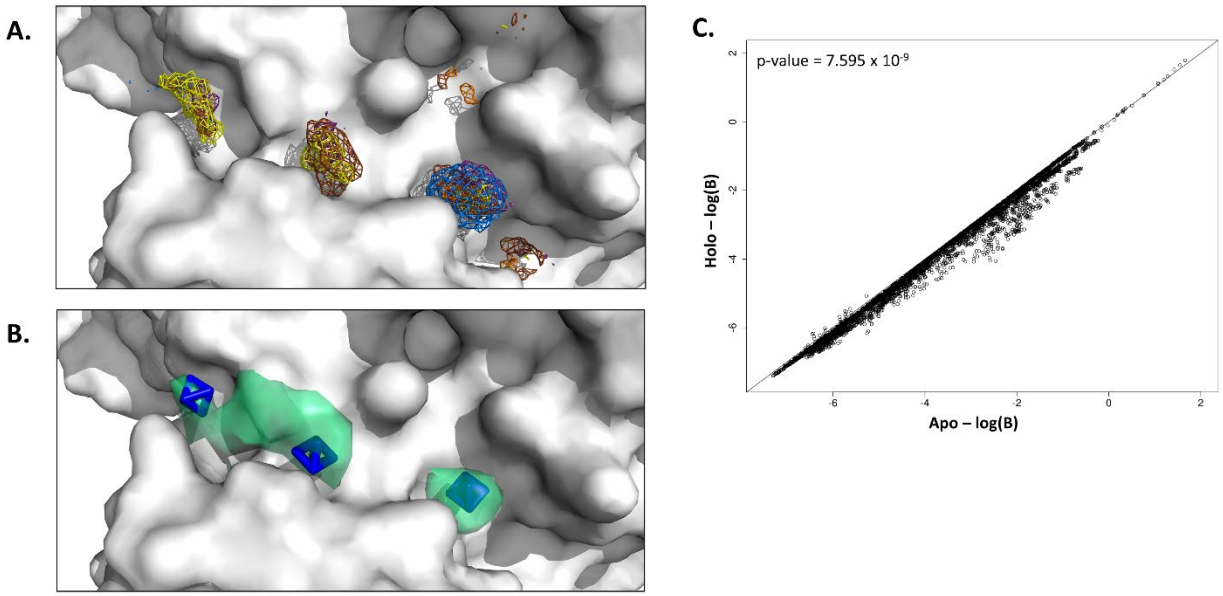

Figure S2. Normal Mode Analysis of Site 1. (A.) A probe occupancy map is shown for pyrimidine (purple), acetonitrile (orange), isopropyl alcohol (blue), ethanol (white), imidazole (brown), and N-methylacetamide (yellow). (B.) Sites 1A, 1B, and 1C were combined into Site 1. Three octahedrons (blue) were placed into each of the predicted sites (green surfaces). (C.) Normal mode analysis was carried out on the apo and holo states of the main protease using the first ten non-redundant modes. Predicted temperature factors were calculated, and a very significant difference was observed between states.

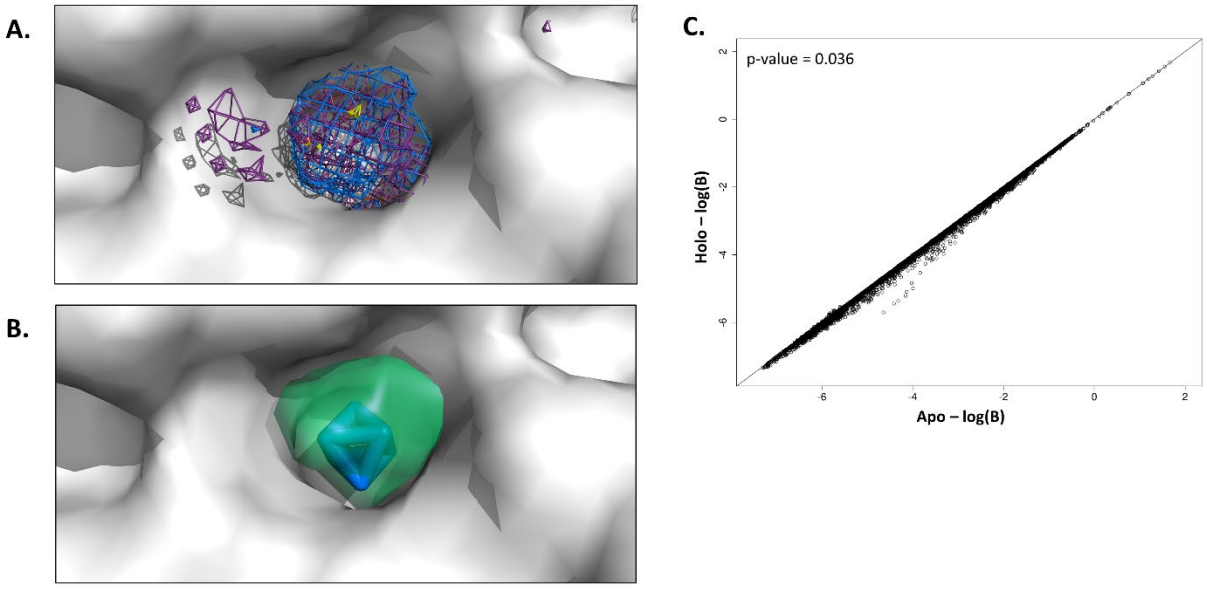

Figure S3. Normal Mode Analysis of Site 2. (A.) A probe occupancy map is shown for pyrimidine (purple), acetonitrile (orange), isopropyl alcohol (blue), ethanol (white), imidazole (brown), and N-methylacetamide (yellow). (B.) A single octahedron (blue) was placed into the predicted sites (green surface). (C.) Normal mode analysis was carried out on the apo and holo states of the main protease using the first ten non-redundant modes. Predicted temperature factors were calculated, and a significant difference was observed between states.

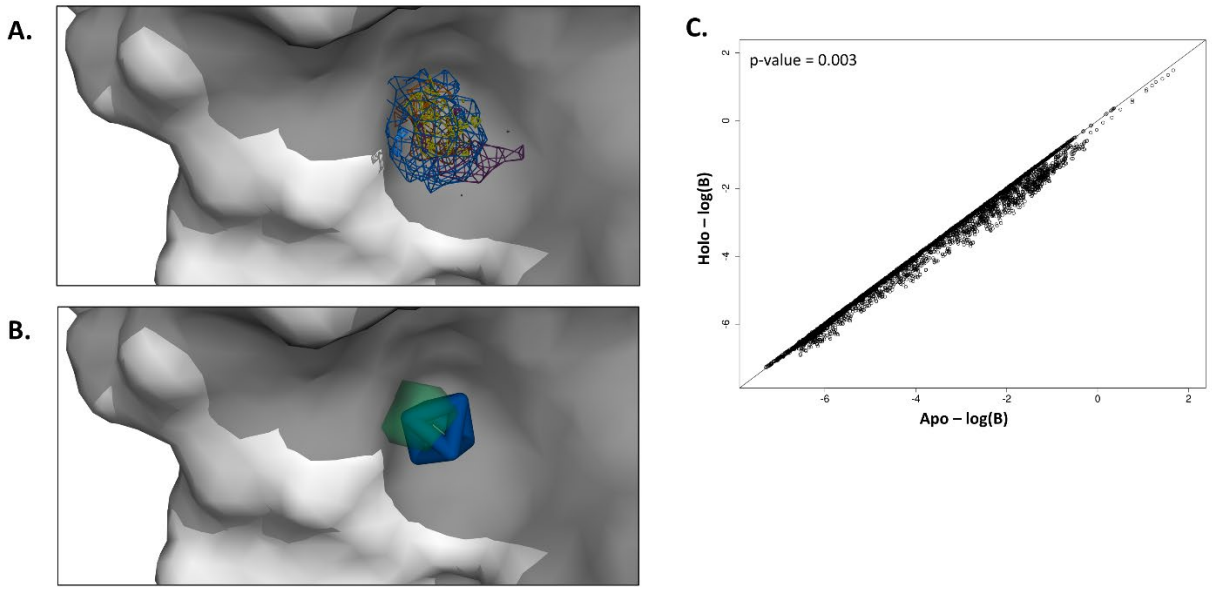

Figure S4. Normal Mode Analysis of Site 3. (A.) A probe occupancy map is shown for pyrimidine (purple), acetonitrile (orange), isopropyl alcohol (blue), ethanol (white), imidazole (brown), and N-methylacetamide (yellow). (B.) A single octahedron (blue) was placed into the predicted sites (green surface). (C.) Normal mode analysis was carried out on the apo and holo states of the main protease using the first ten non-redundant modes. Predicted temperature factors were calculated, and a very significant difference was observed between states.

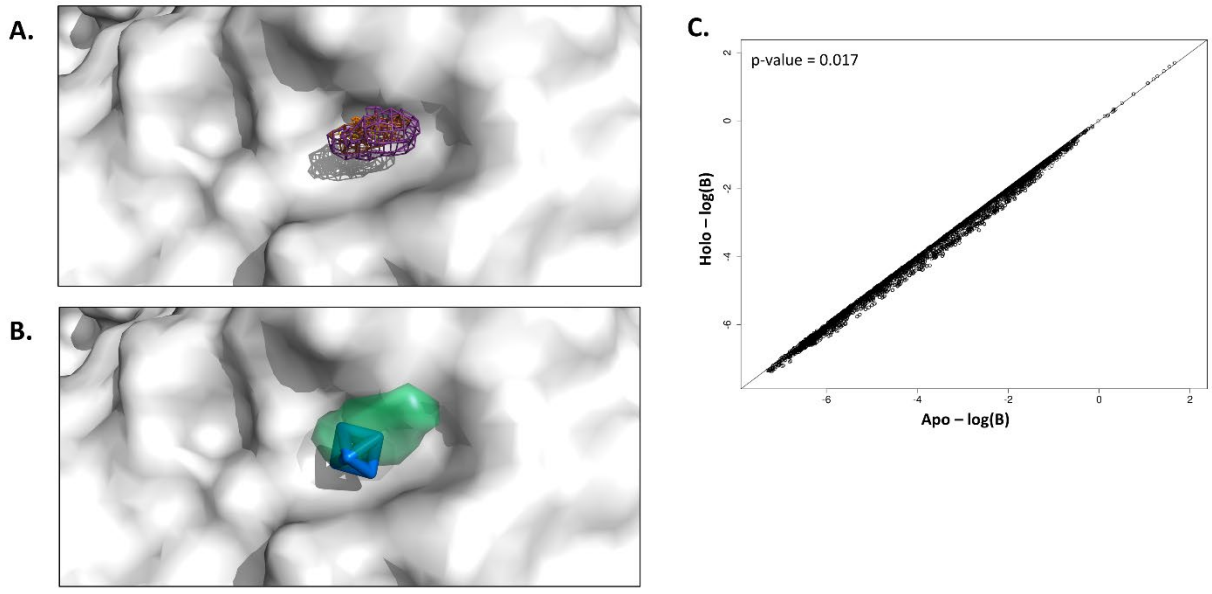

Figure S5. Normal Mode Analysis of Site 4. (A.) A probe occupancy map is shown for pyrimidine (purple), acetonitrile (orange), isopropyl alcohol (blue), ethanol (white), imidazole (brown), and N-methylacetamide (yellow). (B.) A single octahedron (blue) was placed into the predicted sites (green surface). (C.) Normal mode analysis was carried out on the apo and holo states of the main protease using the first ten non-redundant modes. Predicted temperature factors were calculated, and a significant difference was observed between states.

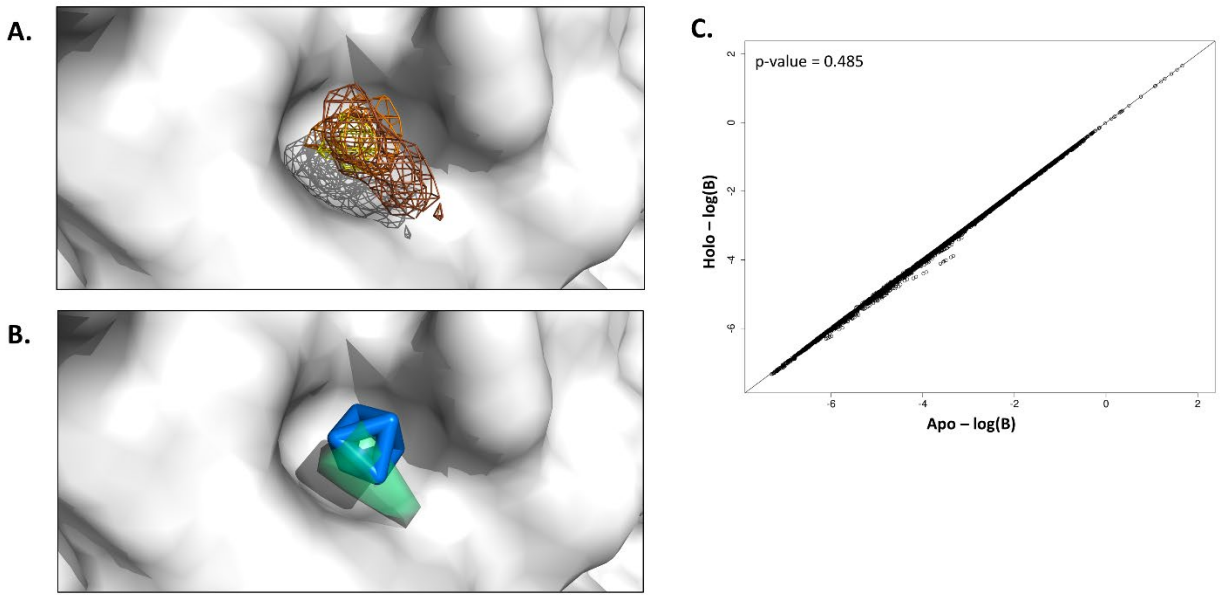

Figure S6. Normal Mode Analysis of Site 5. (A.) A probe occupancy map is shown for pyrimidine (purple), acetonitrile (orange), isopropyl alcohol (blue), ethanol (white), imidazole (brown), and N-methylacetamide (yellow) (B.) A single octahedron (blue) was placed into the predicted sites (green surface). (C.) Normal mode analysis was carried out on the apo and holo states of the main protease using the first ten non-redundant modes. Predicted temperature factors were calculated, and no significant difference was observed between states.

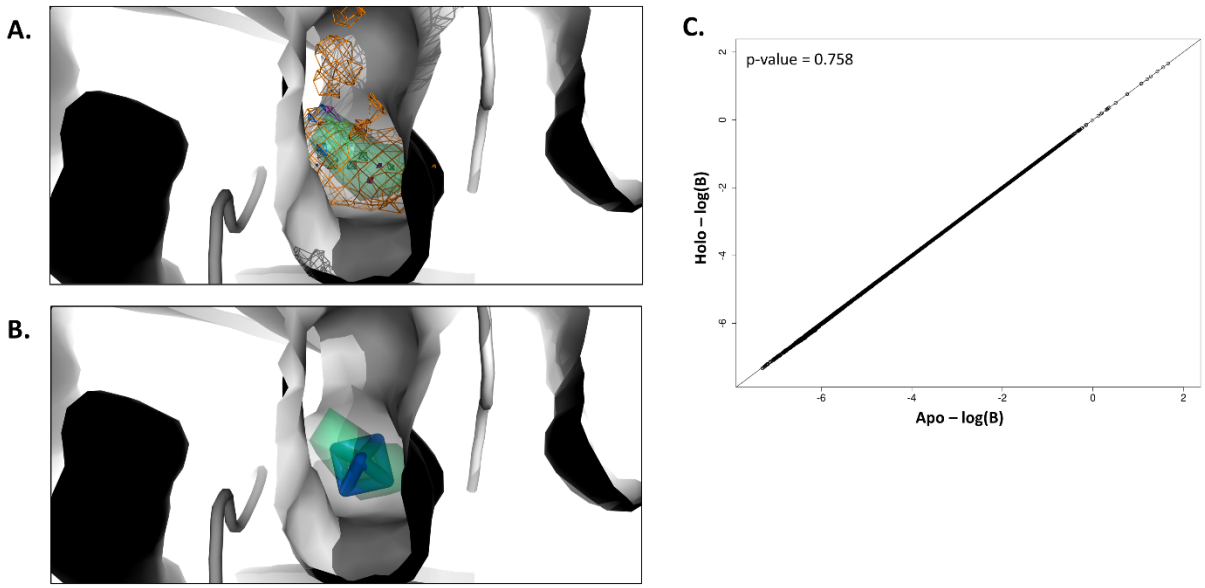

Figure S7. Normal Mode Analysis of Site 6. (A.) A probe occupancy map is shown for pyrimidine (purple), acetonitrile (orange), isopropyl alcohol (blue), ethanol (white), imidazole (brown), and N-methylacetamide (yellow). (B.) A single octahedron (blue) was placed into the predicted site (green surface). (C.) Normal mode analysis was carried out on the apo and holo states of the main protease using the first ten non-redundant modes. Predicted temperature factors were calculated, and no significant difference was observed between states.

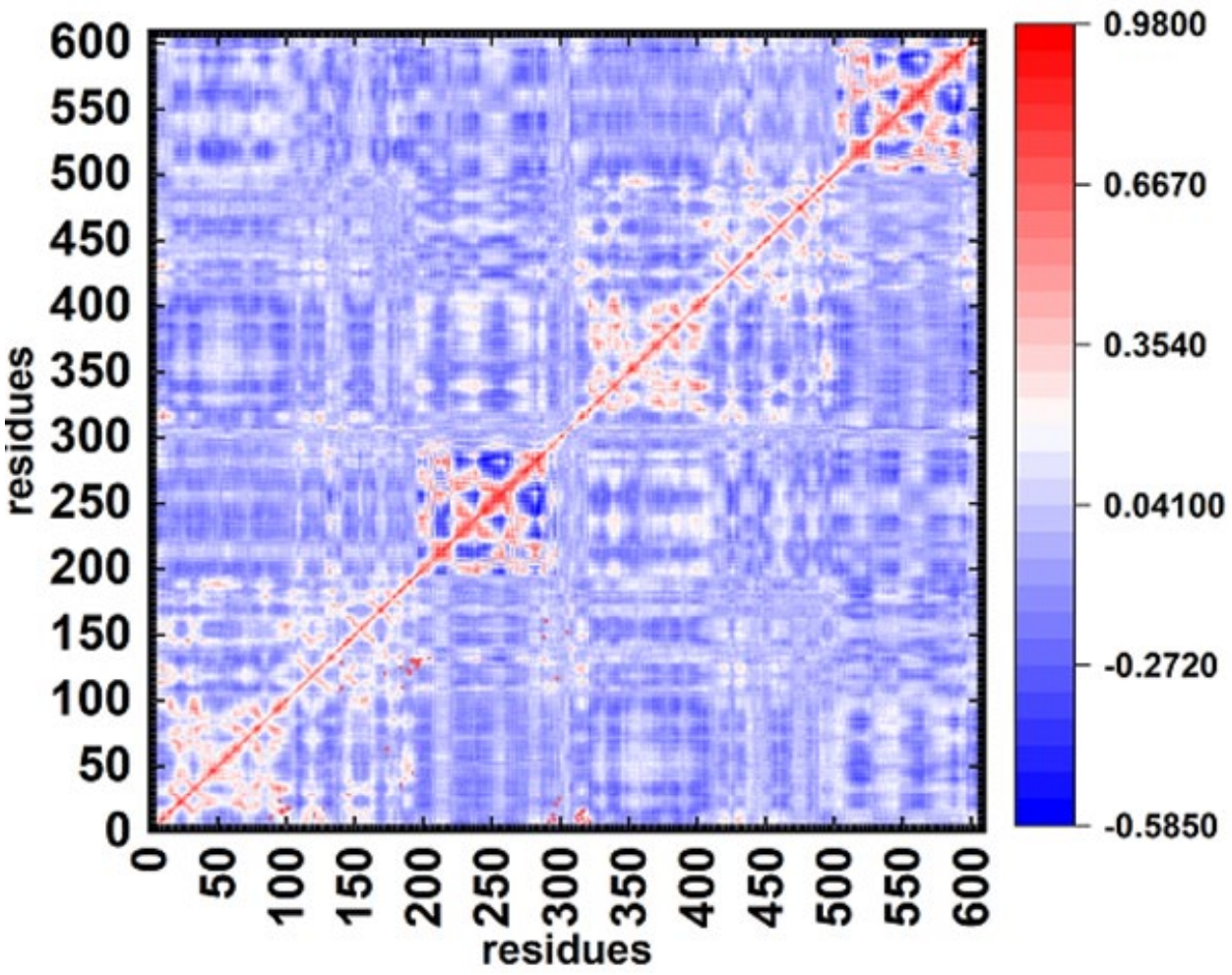

Figure S8. Dynamic cross-correlation plot of the pyrimidine MixMD trajectory. Correlations >0.5 between allosteric-site residues and active-site residues are listed below.

Allosteric-site residues	**Active-site residues**
Site 1 residues 107-109,200-202,251-253,294-297	5,6,7,8,41-44, 140-145,186-189,141-144
Site 2 residues 3,118	5-8, 25-28
Site 2 residues 213,214,299	4-8, 24-27,140-142
Site 3 residues 271,272,275-277	4-8, 24, 25, 27, 41, 43, 44,186-189

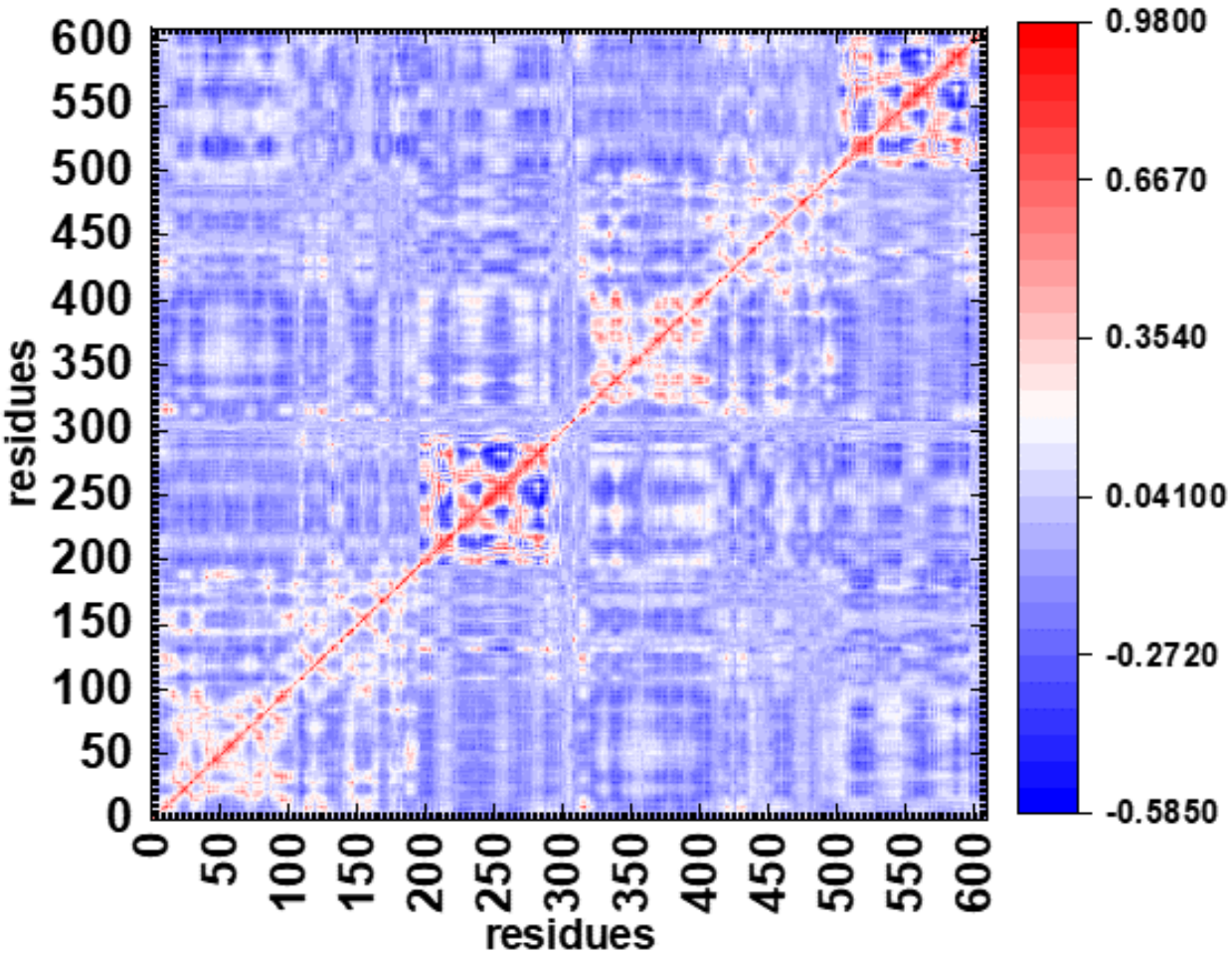

Figure S9. Dynamic cross-correlation plot of the isopropanol MixMD trajectory. Correlations >0.5 between allosteric-site residues and active-site residues are listed below.

Allosteric-site residues	**Active-site residues**
Site 1 residues 107-109	4-8, 110-114, 160-165
Site 1 residues 200-202	4-8,130-144
Site 2 residues 107	4-8,25-28
Site 2 residues 118	4-8, 25-28, 115-120, 141-144
Site 2 residues 140	141-145, 160-165
Site 3 residues 271,272,275-277	No correlations

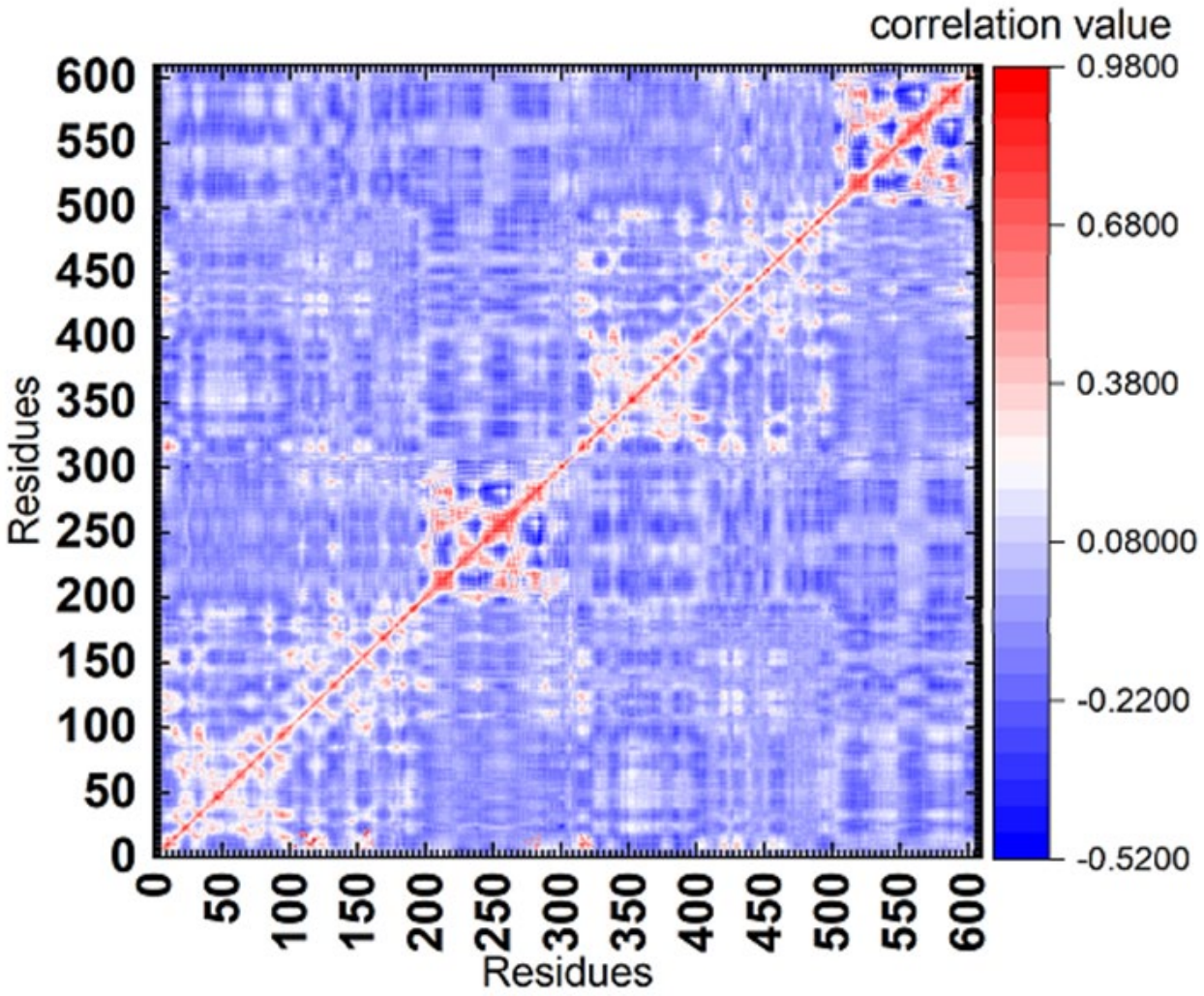

Figure S10. Dynamic cross-correlation plot of the acetonitrile MixMD trajectory. Correlations >0.5 between allosteric-site residues and active-site residues are listed below.

Allosteric-site residues	**Active-site residues**
Site 1 residues	No correlations
Site 2 residues	No correlations
Site 3 residues 217,272,275-277	4-8, 24-27, 43,44

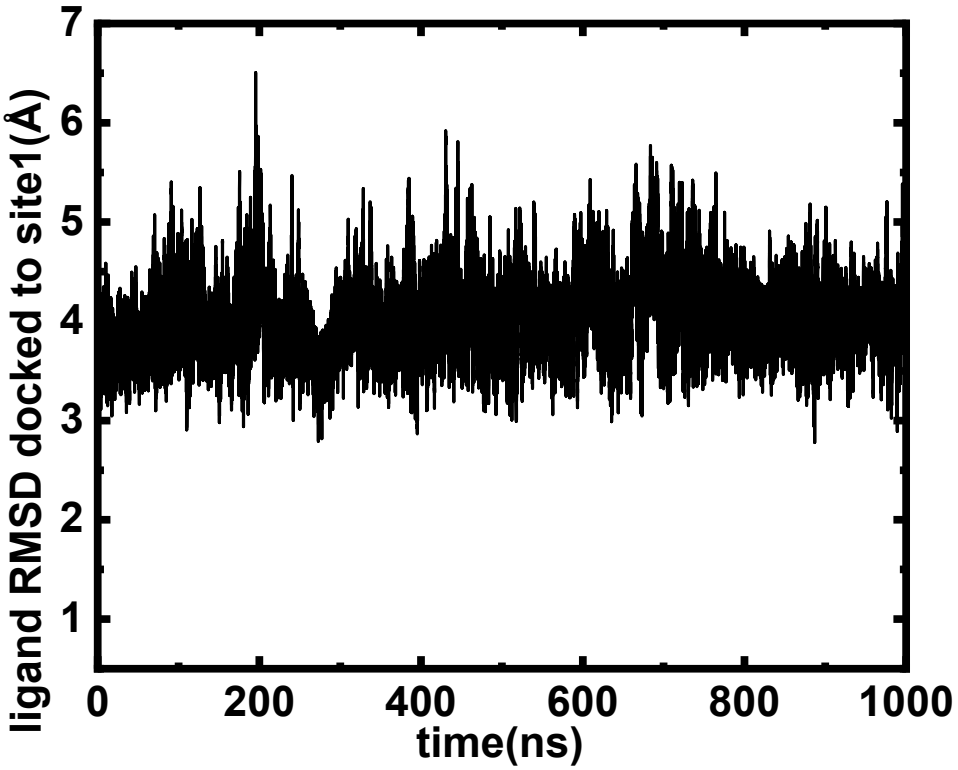

Figure S11. Best binder of allosteric site 1 (Micafungin) RMSD fluctuations as a function of time. RMSD is measured with respect to the initial docked pose of the ligand.

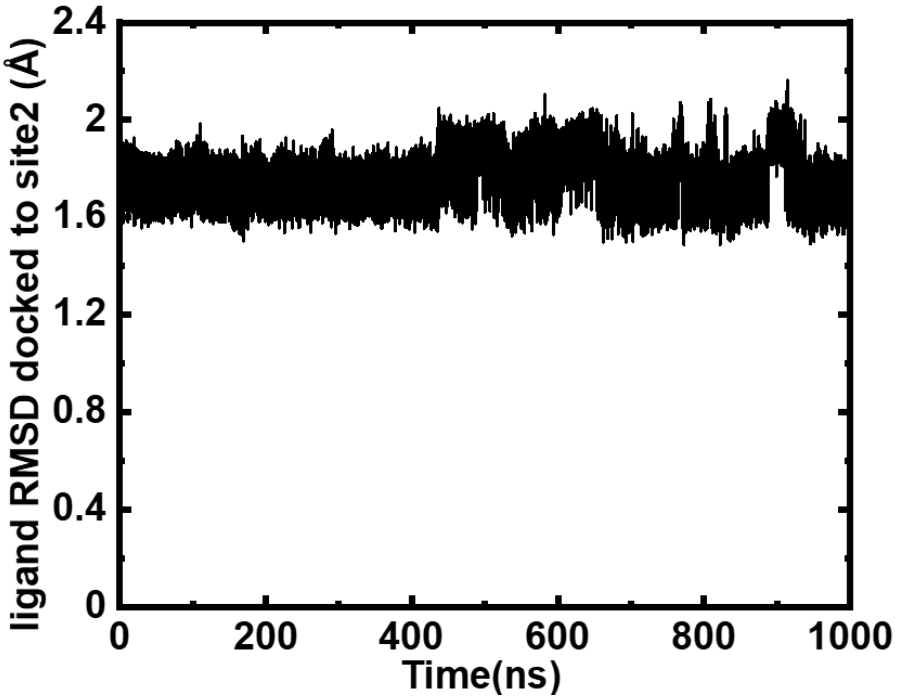

Figure S12. Best binder of allosteric site 2 (NCGC00186009-04) RMSD fluctuation as a function of time. RMSD is measured with respect to the initial docked pose of the ligand.

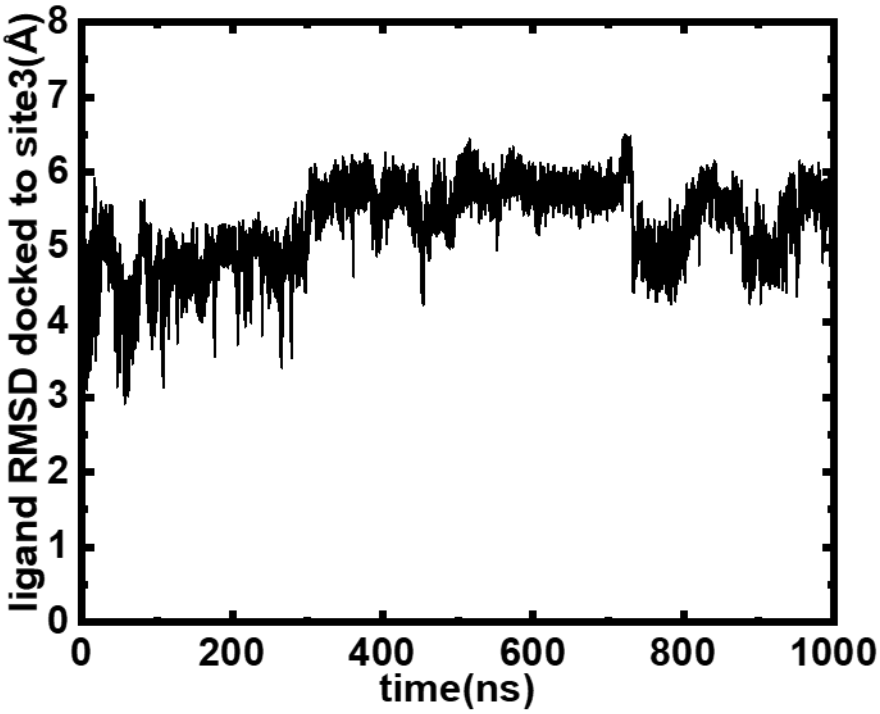

Figure S13. Best binder of allosteric site 3 (Polymyxcin) RMSD fluctuation as a function of time. RMSD is measured with respect to the initial docked pose of the ligand.

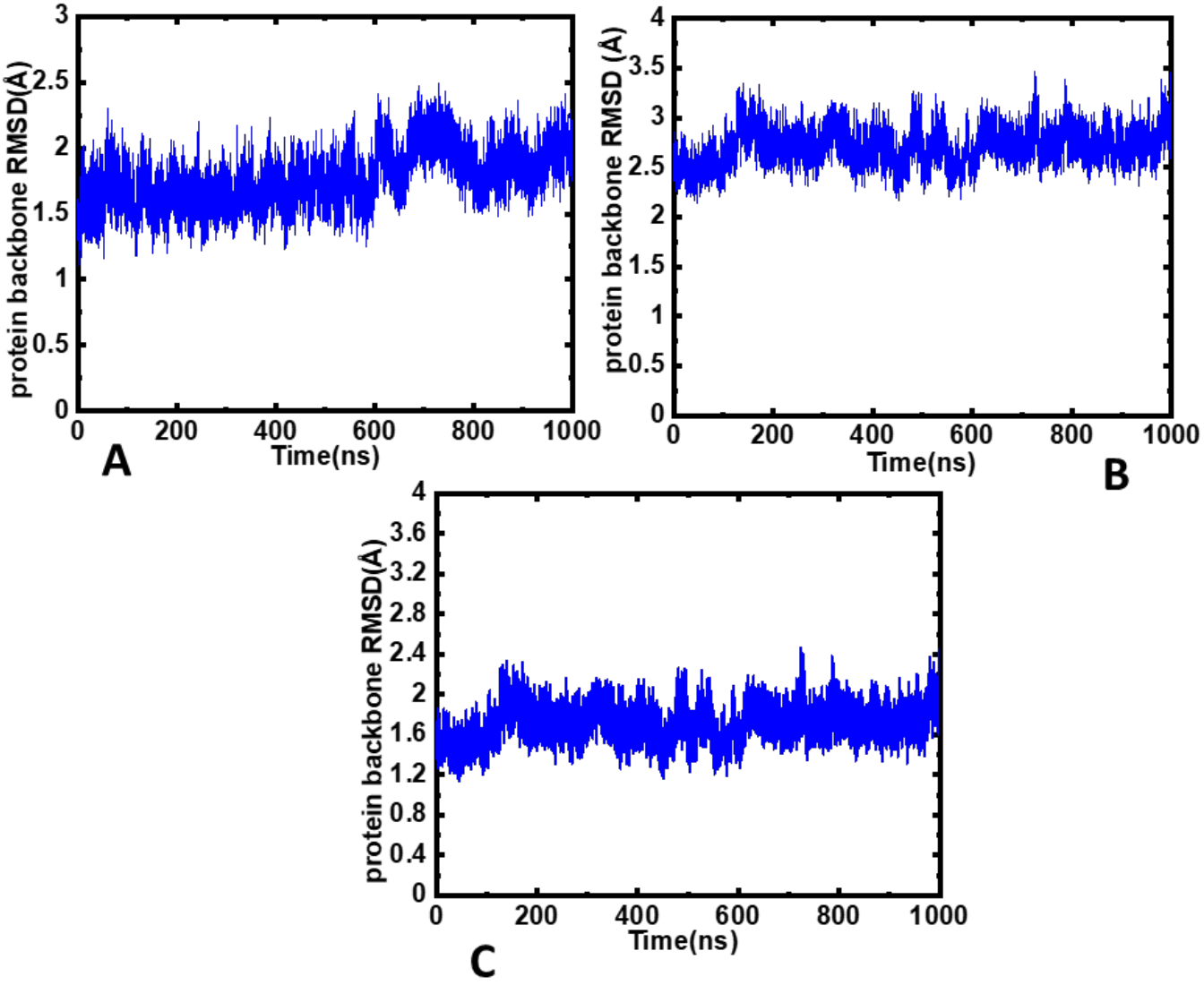

Figure S14. Protein backbone RMSD fluctuations plotted during the 1μs simulations of the allosteric-site binders in (A) site 1, (B) site 2, and (C) site 3.